

Mechanistic Insights into Formic Acid Dehydrogenation and Carbon dioxide Amidation Using Electrophilic Ru(II)-Complexes

Rahul Kumar ^{a*}

^aDepartment of Inorganic and Physical Chemistry, Indian Institute of Science, Bangalore 560 012, India.

e-mail: rkiisc@gmail.com

Abstract: The [RuCl(dppe)₂][OTf] (**1**) complex dehydrogenates formic acid under ambient conditions and results in the formation of *trans*-[Ru(η²-H₂)Cl(dppe)₂][OTf] (**2**) and *trans*-[Ru(η²-H₂)H(dppe)₂][OTf] (**3**) complexes. Addition of sodium formate to this reaction mixture increased the rate of formic acid dehydrogenation and complex **3** was obtained as the final product. Furthermore, complex **1** dehydrogenates formic acid catalytically in the presence of Hunig base. After several catalytic cycles, quantitative amounts of H₂ and CO₂ were produced at 298 K. The proposed formate bound intermediates *cis*-[η²-Ru(HCO₂)(dppe)₂] were too unstable to be observable (or isolable), however, an analogous *cis*-[Ru(η²-CF₃CO₂)(dppe)₂][OTf] complex (**6**) was synthesized and characterized. This complex also dehydrogenates formic acid and led to the formation of complex **3**. Based on NMR spectroscopic studies and other related chemical reactions, a plausible mechanism for formic acid dehydrogenation using complex **1** has been proposed. Moreover, ¹³C NMR spectral data on transfer hydrogenation of CO₂ using complex **1** in presence of tert-butyl amine-borane (TBAB) as a secondary hydrogen source resulted in the amidation of CO₂ to tert-butyl formamide.

Introduction

Water is considered as a cheap and abundant source of hydrogen, however, release of hydrogen from water is not economically viable using currently available technologies.[1–4] In addition, hydrogen storage in the solid state using molecular hydrides such as ammonia-borane (H₃N·BH₃, AB) is being investigated thoroughly from the standpoint of hydrogen release under different conditions.[5,6] However, regeneration of AB from its dehydrogenated by-products, BNH_x polymers is quite challenging. [5,6] Liquid organic hydrides such as formic acid (FA) which could be obtained from biomass in large amounts, has been considered as an attractive choice as hydrogen storage material[7–10] for non-mobile applications where the low wt% hydrogen content is acceptable. Importantly, its dehydrogenation is highly favorable thermodynamically ($\Delta G^\circ = -33$ kJ/mol) and the free energy for its conversion to hydrogen (H₂) and carbon dioxide (CO₂) is quite low ($\Delta G^\circ = 4$ kJ/mol) in aqueous phase.[11–14] Recent research interest in this small organic molecule resulted in the development of numerous homogeneous dehydrogenation catalysts. [7–

10][15–18][19][20][10,13,18,19,21–41][42] Many of these reported catalysts are Ru and Fe metal complexes which dehydrogenate formic acid/formate very efficiently.[10,17,18,19,21,24,26,27,30,33,34,36,38][43] For example, Beller and co-workers developed iron-based homogeneous catalyst which dehydrogenates HCO_2H very efficiently under ambient conditions using eco-friendly solvents without any base additives. They spectroscopically characterized formate bound complexes such as $[\text{Fe}(\eta^2\text{-HCO}_2)(\text{PP}_3)]^+$ or $[\text{Fe}(\text{H})(\eta^1\text{-HCO}_2)(\text{PP}_3)]$ as key intermediates in the catalytic cycle $[\text{PP}_3 = (\text{P}(\text{CH}_2\text{CH}_2\text{PPh}_2)_3)]$ [18]. Also, it was proposed the possibility of formic acid bound intermediate $[(\text{PP}_3)\text{Fe}(\text{HCO}_2\text{H})]$ formed when $\text{Fe}(\text{BF}_4)_2 \cdot 6\text{H}_2\text{O} / \text{PP}_3$ was mixed with formic acid.[18][44] Furthermore, there have been several reports of mechanistic studies on active Ru-catalysts for efficient H_2 production from formic acid and the proposed formate bound ruthenium complexes $[(\text{HCO}_2)\text{RuL}]$ ($\text{L} =$ phosphine, amine based ligands) as intermediates during catalysis.[26,33,36,38,45] Although there has been vast literature on formic acid dehydrogenation using molecular complexes as homogeneous catalysts,[7–10][15–18][19][20][10,13,18,19,21–41][42][43], it is imperative to characterize the key intermediates with intricate structural details such as its η^2/η^1 binding modes to further understand the hydrogen elimination pathways from metal bound formic acid/formate. For examples, Gonsalvi and co-workers reported intermediates such as formato, $[\text{Ru}(\kappa^3\text{-triphos})(\text{MeCN})(\eta^2\text{-HCO}_2)]$ and diformato complex, $[\text{Ru}(\kappa^3\text{-triphos})(\eta^1\text{-HCO}_2)(\eta^2\text{-HCO}_2)]$ in the dehydrogenation of formic acid using Ru-complexes ligated with triphos.[36] In this context, further investigation of the mechanistic details of FA dehydrogenation would be beneficial for the development of finely tuned efficient catalytic systems of the next generation. Moreover, together with carbon dioxide conversion to formic acid, a sustainable cycle for hydrogen storage and release can be envisaged.[17][47]

22 CO_2 is a greenhouse gas, and its continuous rise in concentration (from ~280 ppm of pre-industrial era to ~417 ppm in 2021), and venting ~35 GT per year into the atmosphere would lead to devastating effect of global warming.[48][49][50] Therefore, capture of CO_2 and its recycling via CO_2 activation and subsequent transformation into liquid fuels or useful C1 or C2 feedstock chemicals have become global research objectives for the past few decades.[11,12,14,47,51–56][57–66][67][68][69][70][46] The gas phase reaction of CO_2 and H_2 to HCO_2H has a high positive ΔG° value ($\Delta G^\circ = +33 \text{ kJ/mol}$) because of an entropic contribution; however, formation of formate is more favorable in aqueous ammonia solution ($\Delta G^\circ = -9.5 \text{ kJ/mol}$).[46] Thus, hydrogenation of CO_2 in the gas phase at high temperature and pressure is energy intensive process, and hence it cannot be considered energetically and economically viable for large scale industrial applications for the production of C1 or C2 feedstock chemicals or fuels. On the other hand, transfer hydrogenation is quite simple yet a very powerful method for the synthesis of various hydrogenated

compounds.[71–73][66,67,68–75, 76] Transfer hydrogenation of CO₂ using secondary hydrogen carriers such as amine-boranes into FA (or its derivative, formamides) could be efficient strategies to surpass these bottlenecks. Though transfer hydrogenation is well studied, it has not been investigated thoroughly for CO₂ reduction. Recent studies by Stephan and co-workers on transfer hydrogenation of CO₂ using amine-boranes and frustrated Lewis pairs[85,86] have been inspiring to further investigate the intricate mechanistic details involved in these reactions.

Previously, Ru-complexes reported for catalytic FA dehydrogenation were mostly six-coordinated and octahedral in geometry [26,33,36,38,45,46]; however, Pan et al. recently reported a highly active five coordinated Ru-complex bearing a dearomatized pyridine moiety and an imine arm.[87] Herein, we present the mechanistic insights into FA dehydrogenation by an electrophilic, coordinatively unsaturated Ru-complex, [RuCl(dppe)₂][OTf] (**1**) (a pre-catalyst), having a distorted *trigonal bipyramidal* (tbp) geometry with chelating phosphine ligand (1,2-bis(diphenylphosphinoethane) (dppe)).[88] Interestingly, despite being coordinatively unsaturated and electrophilic Ru-center, complex **1** dehydrogenated FA although at a slow rate, yet under ambient conditions and without any base. Thus, it not only offers further opportunities to explore the detailed kinetics but also to find the intricate details on formic acid/formate binding to Ru(dppe) fragment. For example, complex **1** reacts with silver trifluoroacetate (AgCO₂CF₃) and results in the formation of *cis*-[Ru(η²-CF₃CO₂)(dppe)₂][OTf] (**6**) which is structurally similar to the *in situ* generated (proposed) catalyst *cis*-[Ru(η²-HCO₂)(dppe)₂][OTf] formed in the catalytic dehydrogenation of FA by complex **1** in presence of Hunig base (ⁱPrNEt₂). In addition, we briefly discuss the NMR spectroscopic studies on amidation of CO₂ through transfer hydrogenation approach using tert-butyl amine-borane (^tBuH₂N·BH₃, TBAB, as hydrogen and amine source) and complex **1** as pre-catalyst.

Results and discussion

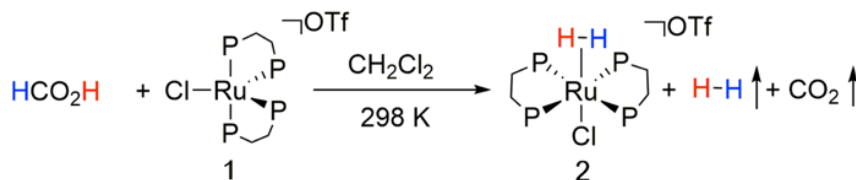
(i) Dehydrogenation of HCO₂H using [RuCl(dppe)₂][OTf] (**1**) and [Ru(η²-CF₃CO₂)(dppe)₂][OTf] (**6**) complexes

(a) Dehydrogenation of HCO₂H by complex **1**

Formic acid (FA), the smallest and the simplest of all carboxylic acids and a liquid under ambient conditions is considered as a very useful organic hydride, highly suitable as hydrogen storage material. By virtue of two distinct hydrogen atoms wherein one is relatively hydridic (–C–H) and other one protic (–O–H) in nature, it is possible to cleave it into its precursor molecules i.e., CO₂ and H₂ (Δ*G*[°] = –33 kJ/mol).[11–14] In addition, it has a low kinetic barrier (~4 kJ/mol) for its dehydrogenation under aqueous conditions.[11–

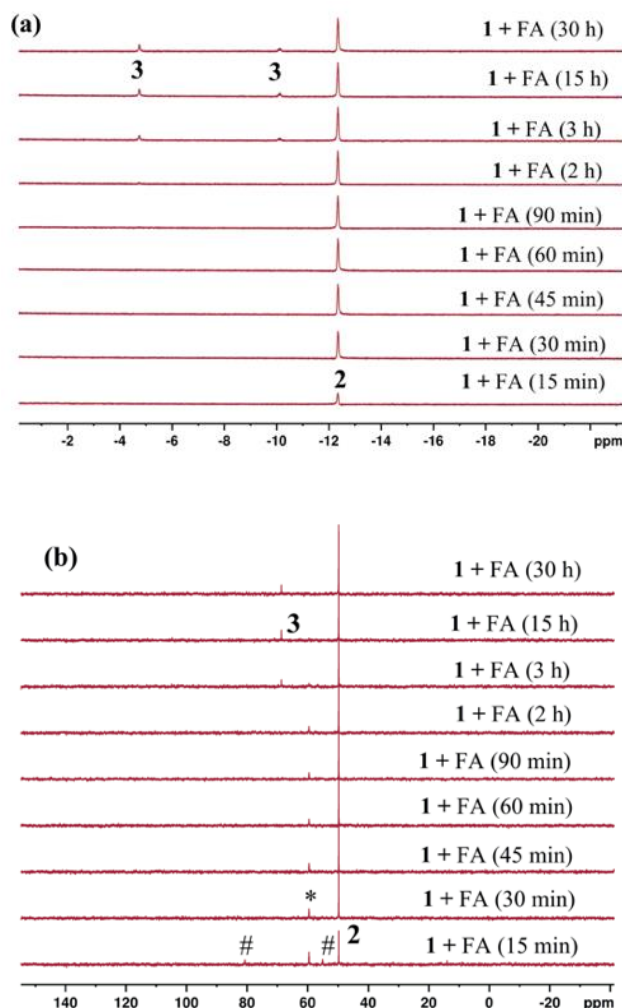
14] It is an electron rich molecule and interacts strongly with highly electrophilic molecules; for example, HCO₂H coordinates to Fe²⁺ in the Beller's catalyst in which the metal ion is surrounded by four chelating phosphines (PP₃ = P(CH₂CH₂PPh₂)₃) and undergoes hydrogen elimination.[18] Previously, we demonstrated that electrophilic, five-coordinated, 16-electron [RuCl(dppe)₂][OTf] complex (**1**) activates the B–H bond in ammonia-borane and related amine-boranes.[89] Complex **1** also undergoes nucleophilic attack of MeLi and leads to the formation of *trans*-[Ru(Me)(Cl)(dppe)₂] complex.[90] Being a relatively mild nucleophile, HCO₂H reacts slowly with complex **1** and resulted in the formation of *trans*-[Ru(η²-H₂)(Cl)(dppe)₂][OTf] (**2**) which showed the characteristic peaks –12.1 ppm for the coordinated dihydrogen and 50.2 ppm for dppe ligand in the ¹H and ³¹P{¹H} NMR spectra, respectively (Scheme 1, Figures 1a-b). [88][89] This ascertained that dehydrogenation of HCO₂H occurs and the evolved hydrogen gas is trapped by complex **1**. The reaction was very apparent by a prominent color change from dark red to orange-red and then to pale yellow. Signals for the dissolved H₂ and CO₂ were observed in the ¹H and ¹³C NMR spectra, respectively (Figure S1). A peak at 59.3 ppm in the ³¹P{¹H} NMR spectrum (Figures 1b) appeared along with complex **2** which slowly disappeared with time; and this signal could be attributed to a formic acid adduct of complex **1** i.e., *trans*-[Ru(HCO₂H)Cl(dppe)₂][OTf] (*) (Figure 1b and see proposed mechanism). Although it is known that formate could bind better than formic acid, previous reports also suggested the proposed formic acid bound metal complexes as intermediates.[18][29][44] However, in our studies, possibility of intermediacy of a formato complex such as *trans*-[Ru(η¹-HCO₂)Cl(dppe)₂][OTf] cannot be ruled out; but upon decarboxylation it would produce *trans*-[Ru(H)Cl(dppe)₂] complex (**4**) and not complex **2**. Thus, based on our NMR spectroscopic observation of formation of complex **2** from complex **1** and formic acid reaction (Scheme 1), we propose the intermediate *trans*-[Ru(HCO₂H)Cl(dppe)₂][OTf] (*) as a very likely precursor for complex **2**. It took nearly 30 min for the quantitative conversion of complex **1** into **2** (Figures 1a-b). Though the concentration of **2** was low initially, it increased up to its maximum within 1 h.

Scheme 1. Reaction of complex **1** with formic acid. Note: Complex **1** is unreactive towards O₂, N₂ and H₂O [88]



In addition to complex **2**, we also observed the gradual formation of *trans*-[Ru(η²-H₂)(H)(dppe)₂][OTf] (**3**) complex[89][91] as a minor product (Scheme 1, Figures 1a-b, ¹H and ³¹P{¹H} NMR stack plots). Complex

1 **3** showed distinct signals at -4.6 ppm (broad singlet) for the bound H_2 ligand ($Ru-(H_2)$), -10.5 ppm (quintet,
2 $^2J_{HP} \sim 20$ Hz) for $Ru-H$ in the 1H NMR and 68.8 ppm (singlet) for dppe ligand in the $^{31}P\{^1H\}$ NMR spectrum
3 (Scheme 1, Figures 1a-b).



4
5
6 **Figure 1.** Partial (a) 1H NMR, (b) $^{31}P\{^1H\}$ NMR spectral stack plots with time showing formation of
7 complexes **2** and **3** in the reaction of complex **1** (#) with formic acid at 298 K in CD_2Cl_2 , * = $trans$ -
8 $[Ru(HCO_2H)Cl(dppe)_2][OTf]$, FA = Formic acid

9 Stirring the reaction mixture for over two days did not result in further conversion of complex **2** to **3**.
10 However, adding sodium formate to the reaction mixture resulted in the complete conversion of **2** to **3** after
11 1h of its addition (Scheme 2 and Figures 2a-b). Though it is not clear as to how the formate anion could
12 help in this transformation, it is plausible that sodium formate traps the proton of complex **2** (because it is
13 acidic, $pK_a \sim 6$)[88]) with concomitant formation of NaCl. The resulting five-coordinate, highly reactive,
14 unobserved $[RuH(dppe)_2][OTf]$ (I^*)[89] species reacts with the dissolved hydrogen gas in the solution

1 leading to the formation of complex **3** (Scheme 2) [89][91]. We demonstrated this transformation at low
 2 temperature earlier using NMR spectroscopy.[89]

3 Scheme 2

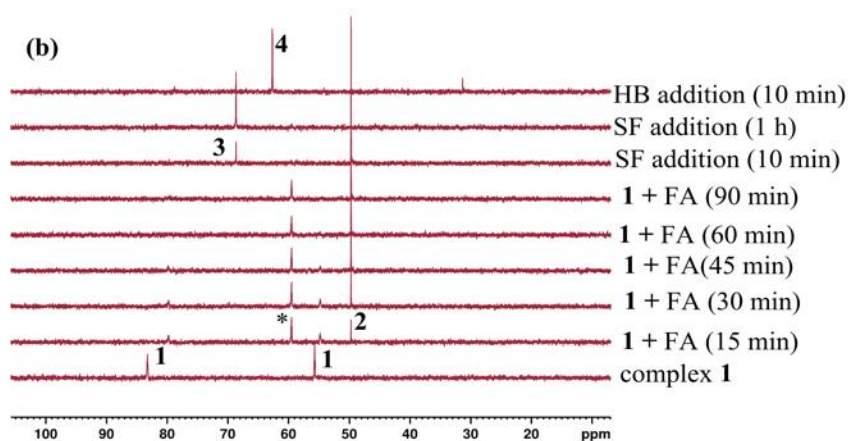
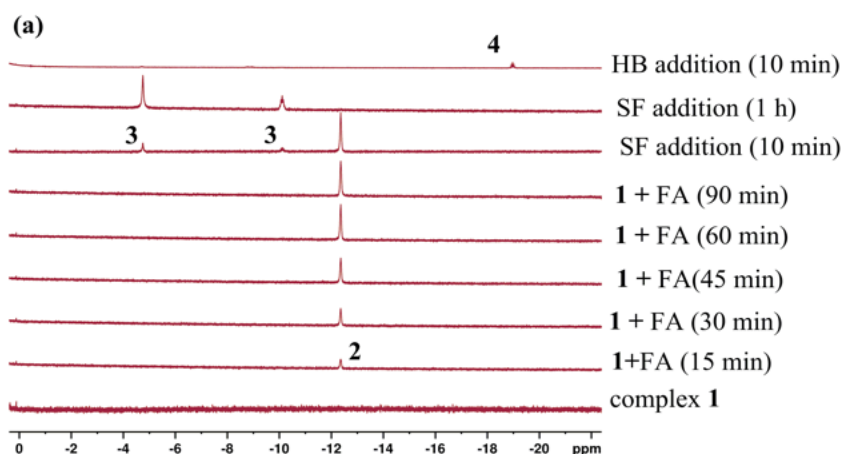
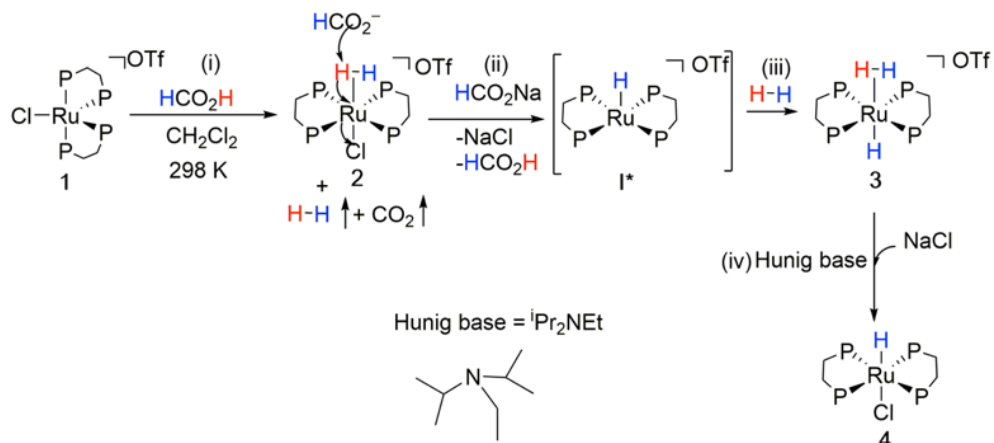
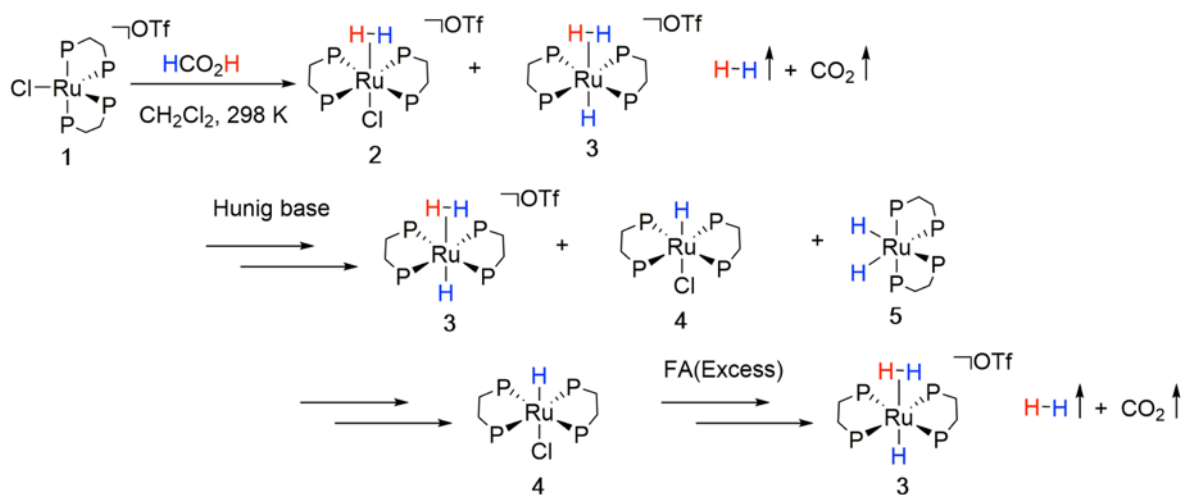


Figure 2. (a) ^1H and (b) $^{31}\text{P}\{^1\text{H}\}$ NMR spectral stack plots with time (SF = sodium formate, HB = Hunig Base) showing formation of complexes **2**, **3** and **4** in the reaction of complex **1** with HCO_2H (FA) at 298 K in CD_2Cl_2 , * = *trans*- $[\text{Ru}(\eta^1\text{-HCO}_2\text{H})\text{Cl}(\text{dppe})_2][\text{OTf}]$

When Hunig base was added to the reaction mixture, dehydrogenation was noted with concomitant formation of *trans*- $[\text{Ru}(\text{H})(\text{Cl})(\text{dppe})_2]$ complex (**4**) which shows a quintet at -18.9 ppm ($^2J_{\text{HP}} \sim 20$ Hz) and 62.0 ppm in the ^1H and $^{31}\text{P}\{^1\text{H}\}$ NMR spectra, respectively (Scheme 2, Figures 2a-b).[88][89]

Hunig base is a highly reactive proton sponge which traps the available protons in the reaction mixture instantaneously and forms $[\text{HN}^i\text{Pr}_2\text{Et}]\text{Cl}$ (or $[\text{HN}^i\text{Pr}_2\text{Et}]\text{OTf}$ or $[\text{HN}^i\text{Pr}_2\text{Et}][\text{HCO}_2]$); then $[\text{HN}^i\text{Pr}_2\text{Et}]\text{Cl}$ would serve as a source of Cl^- and reacts with complex **3** leading to the formation of $[\text{Ru}(\text{H})(\text{Cl})(\text{dppe})_2]$ complex (**4**). As mentioned earlier, complex **1** reacts with HCO_2H slowly, however, in a controlled experiment when $10\ \mu\text{L}$ of Hunig base ($^i\text{Pr}_2\text{NEt}$, HB), was added to the reaction mixture (after ~ 4 h of HCO_2H addition), mild bubbling was observed, which is indicative of dehydrogenation of formate. The rate of bubbling gradually slowed down as the formate concentration dropped down. We recorded the NMR spectral data immediately upon HB addition and the ^1H and $^{31}\text{P}\{^1\text{H}\}$ NMR spectra showed complexes **3** and **4** and a small amount of *cis*- $[\text{RuH}_2(\text{dppe})_2]$ (**5**) which was previously reported by Grubbs. (Scheme 3, Figures 3a-b).[92]

Scheme 3



Although we do not know how complex **5** is forming, however, based on the NMR spectroscopic studies (Figures 3a-b), it is proposed that complex **3** could be the likely precursor which undergoes deprotonation in presence of Hunig base leading to the formation of complex **5**. Moreover, other possible route for the formation of complex **5** such as oxidative addition of H_2 on the $[\text{Ru}(\text{dppe})_2]$ species, cannot be ruled out

completely. Further addition of excess HCO_2H to the reaction mixture resulted in its dehydrogenation and exclusive formation of complex **3** was noted (Scheme 3, Figures 3a-b). The ^{13}C NMR spectrum evidenced complete dehydrogenation of HCO_2H which was apparent from the disappearance of the characteristic signal of HCO_2H upon addition of Hunig base; the evolved H_2 and CO_2 gases were detected by ^1H and ^{13}C NMR spectra, respectively (See SI).

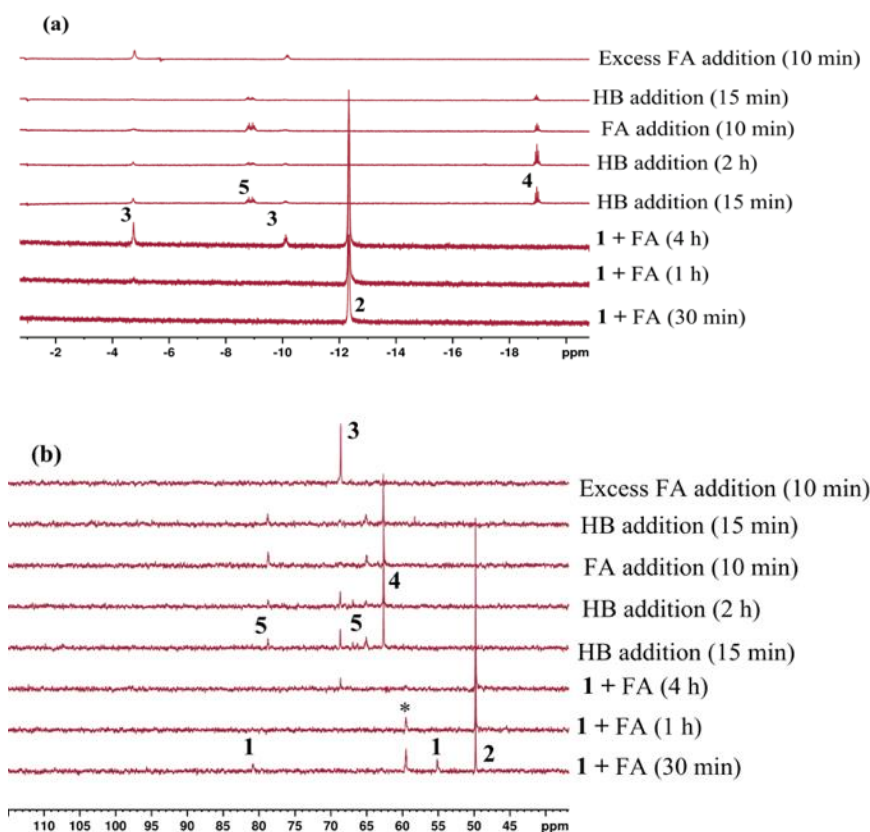


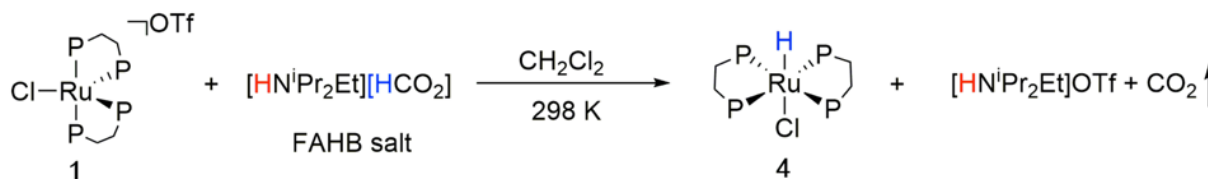
Figure 3. (a) ^1H and (b) $^{31}\text{P}\{^1\text{H}\}$ NMR spectral stack plots with time (and HB or FA additions) showing complexes **2**, **3**, **4** and **5** in the reaction of complex **1** with HCO_2H at 298 K in CD_2Cl_2 , * = *trans*- $[\text{Ru}(\text{HCO}_2\text{H})\text{Cl}(\text{dppe})_2][\text{OTf}]$, FA = Formic acid, HB = Hunig base

Once gas evolution ceased, subsequent addition of more HCO_2H and Hunig base to the reaction mixture resulted in the re-initiation of gas evolution. Therefore, the reaction was tested for four consecutive runs using formic acid-Hunig base salt and each run resulted in gas evolution, indicating catalytic dehydrogenation of HCO_2H by the ruthenium complex. We propose that the pre-catalyst complex **1** generates a highly reactive and active catalyst *in situ* which is tentatively assigned as a formate bound *cis*- $[\text{Ru}(\eta^2\text{-HCO}_2)(\text{dppe})_2][\text{OTf}]$ complex (*vide infra* in proposed mechanism). Furthermore, heating the reaction mixture to 60 °C led to vigorous bubbling indicative of rapid dehydrogenation of formic acid.

The highly reactive *cis*-[(η^2 -HCO₂)Ru(dppe)₂][OTf] proposed catalyst participates in the catalytic dehydrogenation of formic acid only in the presence of Hunig base. After the complete dehydrogenation of HCO₂H by the proposed catalyst *cis*-[Ru(η^2 -HCO₂)(dppe)₂][OTf], exclusive formation of complex **3** (in presence of excess FA) or **4** (in presence of excess HB) as final products were observed in the ¹H and ³¹P{¹H} NMR spectra (Figures 3a-b and vide infra proposed mechanism). The proposed active catalyst was not observed under the reaction conditions due to its instability, since it could undergo β -hydride elimination and decarboxylation, and other possible side reactions such as replacement of the bound formate by H₂ or Cl⁻.

To obtain further insight into the mechanism, it is crucial to obtain evidence for the formate bound intermediate. It should be noted that in presence of excess HB, formic acid exists as diisopropyl ethyl ammonium formate anion, [HNⁱPr₂Et][HCO₂], a nucleophile. This species is prone to dehydrogenation/decarboxylation. It could react with complex **1** or complex **2** and result in the formation of the proposed active catalyst (vide infra proposed mechanism). However, when complex **1** was reacted with formic acid and Hunig base salt (obtained from formic acid and Hunig base in 1:1 ratio), it resulted in an instantaneous color change from dark red to yellow and exclusive formation of complex **4** as noted in the ¹H and ³¹P{¹H} NMR spectra (Scheme 4, see SI for spectra). [88][89] This indicates that complex **1** undergoes nucleophilic attack of formate anion leading to the formation of *trans*-[Ru(HCO₂)(Cl)(dppe)₂] as an intermediate. This species undergoes subsequent decarboxylation with a concerted hydride migration (after formyl C–H bond cleavage) resulting in the formation of complex **4** with a *trans* geometry (we cannot rule out the possibility of other pathways which are shown in the SI). This reaction was found to be too rapid that the formate bound intermediate could not be observed.

Scheme 4. Reaction of complex with formic acid and Hunig base (FAHB) salt at 298 K

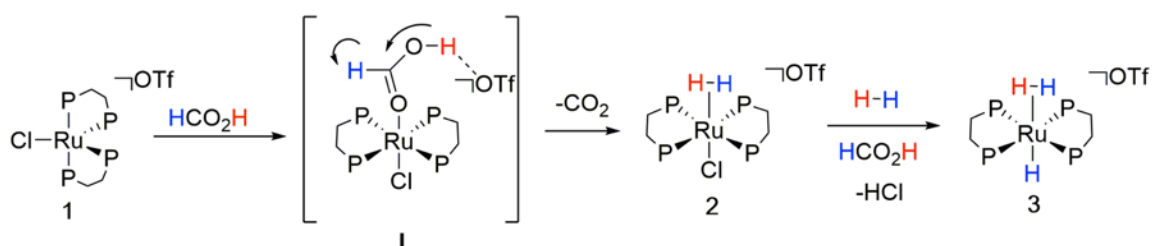


It is to be noted in this reaction that complex **4** was formed exclusively instead of complexes **2** and **3** which is very likely because the proton from formic acid is no more available since it is already trapped by the proton sponge (Hunig base). To further support our proposal of *in situ* generation of catalyst (see proposed mechanism in Scheme 5), a similar reaction of complex **1** with another carboxylate anion, silver trifluoroacetate was carried out independently (Scheme 6); this reaction resulted in an instantaneous color change from dark red to yellow accompanied by the formation of white precipitate. The ¹H, ³¹P{¹H} and

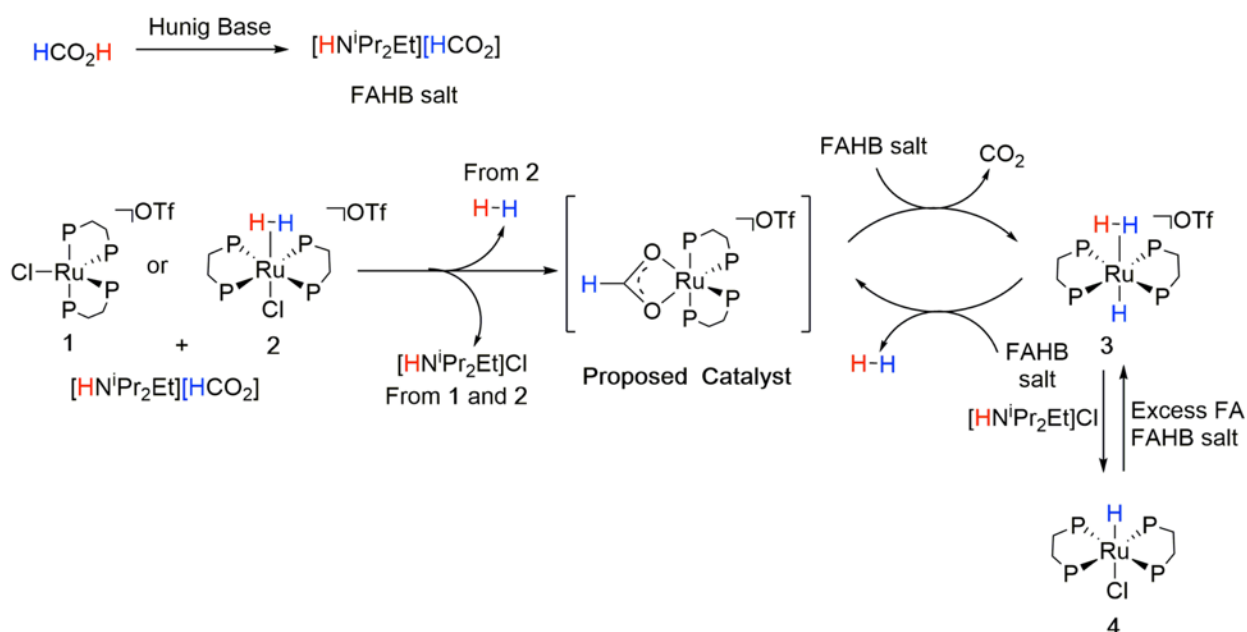
1 ^{19}F NMR spectral data evidenced the formation of a *cis*- $[\text{Ru}(\eta^2\text{-CF}_3\text{CO}_2)(\text{dppe})_2][\text{OTf}]$ complex (**6**)
 2 (Scheme 6, Figure S5 & S6 for NMR spectral data). The $^{31}\text{P}\{^1\text{H}\}$ NMR spectral features corroborate with
 3 a previous literature report[93] and suggest a *cis* geometry for the complex **6**. These observations support
 4 our proposal for the *in-situ* formation of the plausible formate bound catalyst *cis*- $[\text{Ru}(\eta^2\text{-HCO}_2)(\text{dppe})_2][\text{OTf}]$ because it has the same chelating carboxylate anion as a functional group and hence
 5 exhibits same coordination mode as that of formate anion.
 6

7 **Scheme 5.** Proposed mechanism of formic acid dehydrogenation by complex **1**

Proposed mechanism for dehydrogenation of formic acid in absence of a base

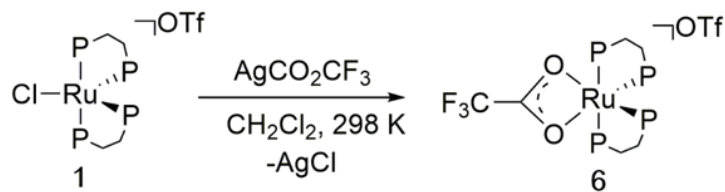


Proposed mechanism for catalytic dehydrogenation of formic acid (FA) in presence of Hunig base (HB)



8

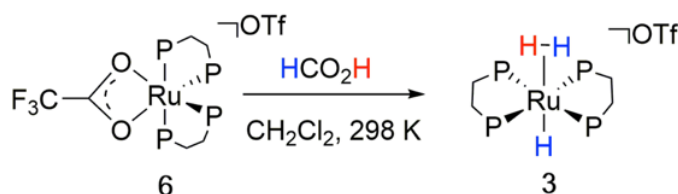
9 **Scheme 6**



(b) Dehydrogenation of HCO₂H by *cis*-[Ru(η²-CF₃CO₂)(dppe)₂][OTf] complex (**6**)

Although complex **6** is quite stable thermodynamically, due to lack of hydrogen atoms on the carboxylate group of coordinated trifluoroacetate, yet the ligand is very labile in nature. Its weakly coordinative property could be attributed to the electron withdrawing nature of CF₃ group and resonance stabilized carboxylate anion. Addition of formic acid (~10 μL) to complex **6** at 298 K resulted in exclusive formation of complex **3** within 40 min (Scheme 7, see SI for NMR spectra). It is interesting to note that this reaction takes place in the absence of any added base. This observation provided some insights into the mechanism of formation of complex **3** from the Ru-formate intermediate.

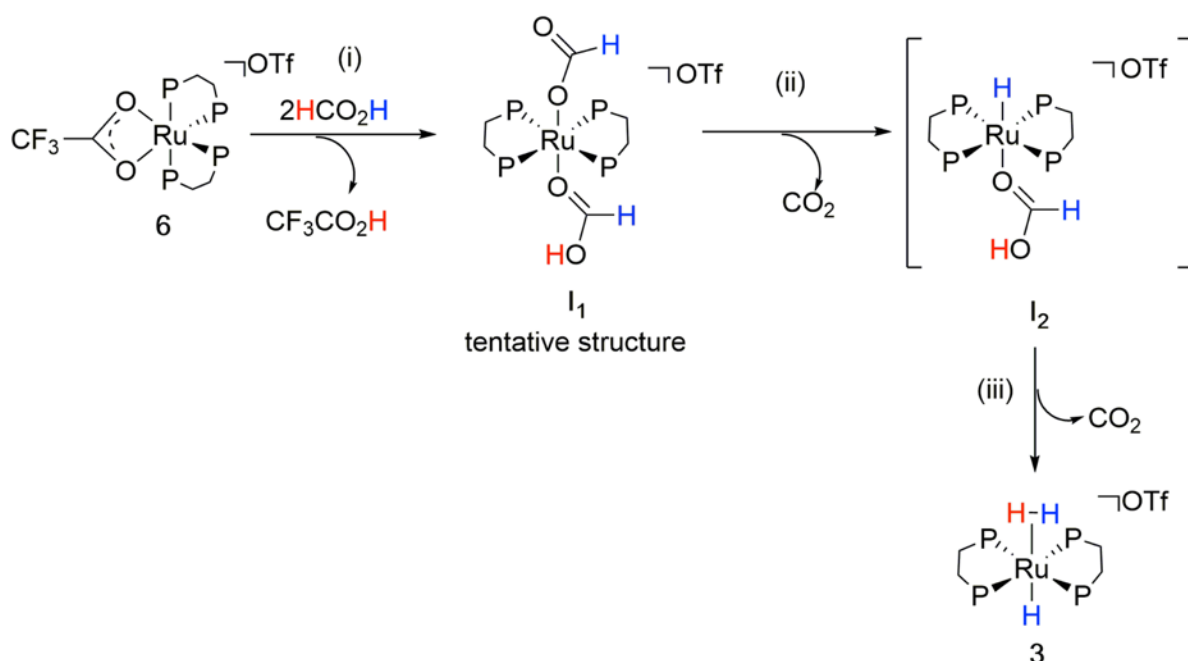
Scheme 7



As formate anion is a better donor than trifluoroacetate ligand, it replaces the weakly coordinated trifluoroacetate which gets eliminated as trifluoroacetic acid (Scheme 8). Furthermore, the possibility of reverse reaction taking place could be considered, since trifluoroacetic acid is more acidic than formic acid. These two reactions could lead to a dynamic equilibrium however, spectral data do not support any such equilibrium process. Thus, it could be envisaged that the replacement of trifluoroacetate ligand by formic acid/formate could occur rapidly precluding the observation of protonation of formate by trifluoroacetic acid. The ³¹P{¹H} NMR spectral stack plot with time showed complete conversion of complex **6** into an intermediate upon addition of formic acid which showed a singlet at 57.0 ppm (see SI) suggesting a trans geometry, and tentatively assigned as *trans*-[Ru(η¹-HCO₂)(HCO₂H)(dppe)₂][OTf] (**I₁**) (Scheme 8). A similar singlet peak was noted at 59.3 ppm in the ³¹P{¹H} NMR spectrum in the dehydrogenation of formic acid by complex **1** along with complex **2** which was ascribed to a similar species with tentative structure *trans*-[Ru(HCO₂H)Cl(dppe)₂][OTf] (**I**) as mentioned earlier (Scheme 5). One of the plausible pathways for dehydrogenation of formic acid by complex **6** is the formation of intermediate **I₁** with concomitant

CF₃CO₂H elimination (Scheme 8, step i). This could further undergo decarboxylation from the bound formate first with formation of an intermediate species (unobserved), *trans*-[Ru(H)(HCO₂H)(dppe)₂][OTf] (**I₂**) (Scheme 8, step ii). The intermediate **I₂** could result in the formation of complex **3** upon decarboxylation (Scheme 8, step iii). Although the dehydrogenation/decarboxylation steps ii and iii could occur either in a stepwise or concerted manner, it could be possible that another pathway involving a competition between formate and formic acid for decarboxylation might exist, which cannot be ruled out (see SI, Scheme S2).

Scheme 8. Proposed mechanism for dehydrogenation of HCO₂H by complex **6**



8

(c) Measurement of evolved H₂ and CO₂ gases from dehydrogenation of HCO₂H by [RuCl(dppe)₂][OTf] complex (1**)**

Complex **1** reacts with formic acid (HCO₂H, 20 μL, 0.52 mmol) slowly and subsequently dehydrogenates/decarboxylates it which was quite evident from the formation of complex **2** and also from the spectroscopically detected dissolved H₂ and CO₂ in the reaction mixture (Figure S1). The measurement of evolved H₂ and CO₂ gases in this reaction yielded very low quantity (~1.4 mL) even after ~30 min (Figure 4, black square curve). When Hunig base (100 μL, 0.6 mmol) was added, rapid dehydrogenation of HCO₂H was noted. In the presence of Hunig base, dehydrogenation/decarboxylation of formic acid proceeded nearly to completion within ~30 min and quantitative amount (~24 mL) of gas was evolved (Figure 4, red circle curve).

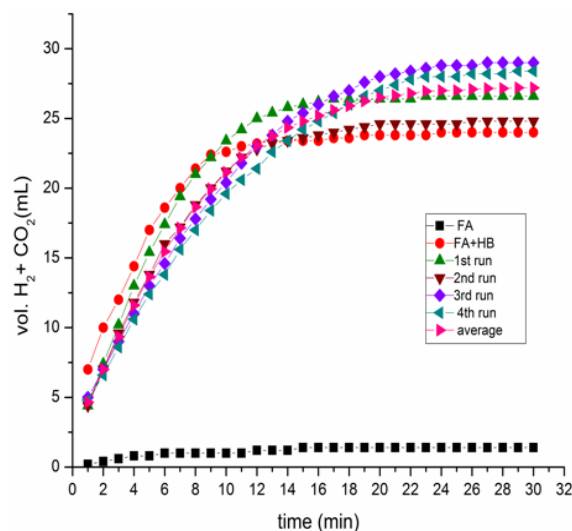


Figure 4. Plot of volume (mL) of $\text{H}_2 + \text{CO}_2$ vs time (min) for catalytic dehydrogenation of formic acid (FA) in presence of Hunig base (HB) by precatalyst **1** in CH_2Cl_2 at 298 K

Subsequently, four consecutive runs of dehydrogenation/decarboxylation were performed by adding formic acid-Hunig base salt and each run yielded quantitative amount (24-29 mL) of $\text{H}_2 + \text{CO}_2$ gas (Figure 4). The average of all four runs plotted in the same graph (Figure 4, pink triangle curve), gave a balanced saturation curve (Figure S3) which prompted us to conclude that complete dehydrogenation/decarboxylation of formic acid (20 μL , 0.52 mmol) had taken place. Within ~ 30 min, the reaction was complete and thus, the overall turnover number (TON) and turnover frequency (TOF) for this reaction after four consecutive runs were calculated to be 416 and 832 h^{-1} , respectively. We also noted that increasing the temperature and amount of formic acid led to vigorous dehydrogenation/decarboxylation.

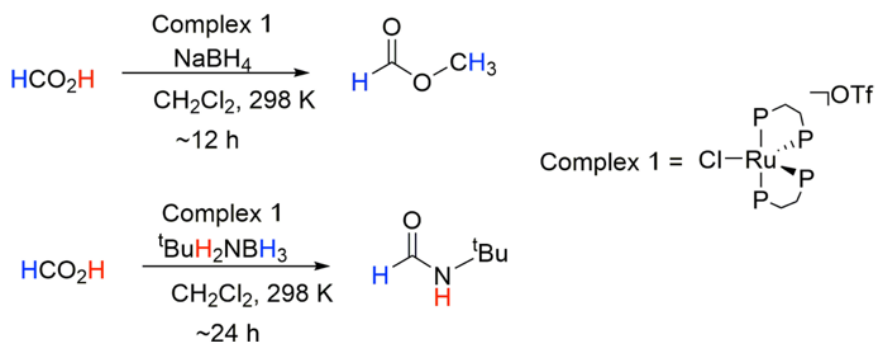
It should be noted that these measurements were carried out using dried and degassed dichloromethane. However, when the catalyst was exposed to air and dichloromethane was not degassed, its decomposition took place after the second run. The pale yellow colored solution changed to green-yellow slowly and finally to dark green solution after several runs. Nevertheless, the dark green solution was found to dehydrogenate/decarboxylate formic acid catalytically and the ^1H and $^{31}\text{P}\{^1\text{H}\}$ spectral data suggest that dppe ligand got oxidized to dppeO and it is accompanied (see Figure S8 & S9) by the formation of an unidentified $\text{Ru}(\text{dppe})$ fragment.

(d) Amidation of CO_2 using tert-butyl amine-borane ($^t\text{BuH}_2\text{N}\cdot\text{BH}_3$, TBAB) using $[\text{RuCl}(\text{dppe})_2][\text{OTf}]$ complex (**1**)

In a pressure stable NMR tube, a reaction of sodium borohydride (NaBH_4) with formic acid (HCO_2H) in presence of complex **1** at 298 K resulted in the formation of methyl formate (Scheme 9). Formation of

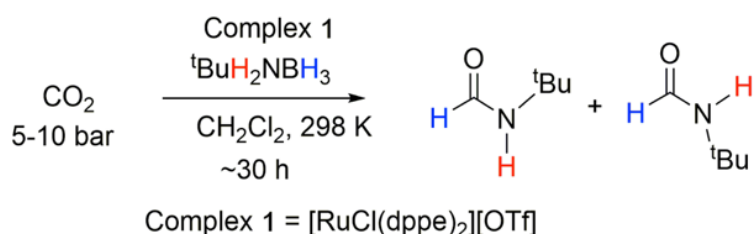
methyl formate ester was confirmed by ^{13}C NMR spectrum (Figure S11). Since the reaction proceeded slowly (~ 12 h), it prompted us to use a soluble primary amine-borane such as tert-butyl amine-borane ($^t\text{BuH}_2\text{N}\cdot\text{BH}_3$, TBAB) as a reducing agent instead of the sparingly soluble NaBH_4 . Considering the solubility and reducing property of TBAB, it was tested for the reduction of formic acid using complex **1** in a pressure stable NMR tube at (Scheme 9). This reaction yielded N-tert-butyl formamide and other carbonyl intermediates (unidentified) signals were noted in the ^{13}C NMR spectrum (Figure S12).

Scheme 9. Reduction and amidation of formic acid



Therefore, similar to formic acid transformation to N-tert-butyl formamide by TBAB, transfer hydrogenation of CO_2 was also carried out using TBAB and complex **1** under ambient conditions. Interestingly, this reaction resulted in the formation of N-tert-butyl formamide which was characterized by ^{13}C NMR spectroscopy (Scheme 10, Figure 5). In addition to signals due to unidentified species, peaks for formyl hydrogen atoms of N-tert-butyl formamide isomers at 7.3 and 8.0 ppm were noted in the ^1H NMR spectrum. The ^1H and $^{31}\text{P}\{^1\text{H}\}$ NMR spectra also showed signals for complexes *trans*- $[\text{Ru}(\eta^2\text{-H}_2)\text{H}(\text{dppe})_2][\text{OTf}]$ (**3**) and *trans*- $[\text{RuHCl}(\text{dppe})_2][\text{OTf}]$ (**4**) (Figure S13).

Scheme 10. CO_2 amidation through transfer hydrogenation using complex **1** and $^t\text{BuH}_2\text{N}\cdot\text{BH}_3$



Note: Transfer hydrogenation of CO_2 to N-tert-butyl formamide was also brought about by the pre-catalyst $[\text{RuCl}_2(\text{PPh}_3)_3]$ in presence of TBAB as secondary hydrogen carrier (Figure S14)

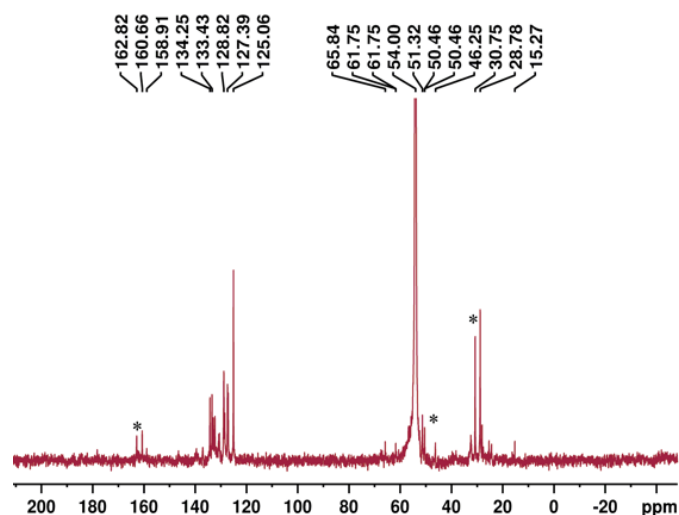


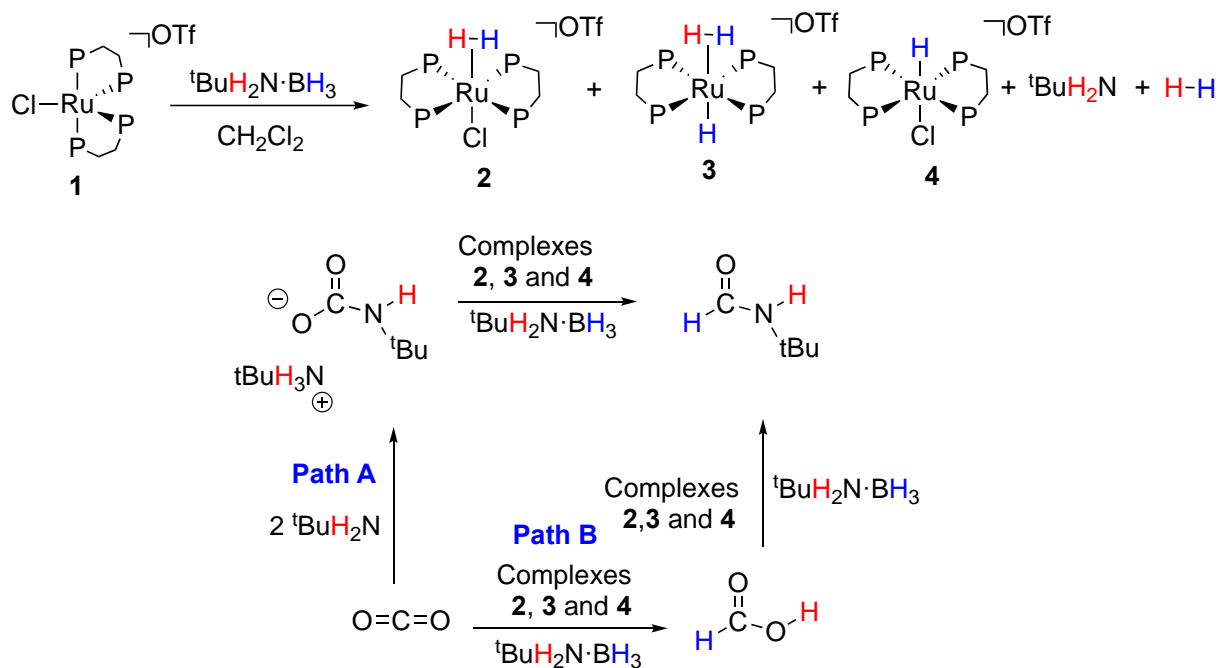
Figure 5. ^{13}C NMR spectrum of the reaction mixture for transfer hydrogenation of CO_2 using TBAB in presence of complex **1** in CH_2Cl_2 at 298 K showing N-tert-butyl formamide (*).

Although several reports on mechanistic studies of CO_2 reduction in presence of amines/phosphines are available in the literature[94][59][95][96][97][52]; reports on transfer hydrogenation of CO_2 using amine-boranes are scarce. [85,86] Sanford *et al.* reported hydrogenation of CO_2 to methanol at 50 bar of H_2 and 155°C in THF using Ru-catalysts in presence of an amine.[94]

Previously, we reported on the rapid dehydrogenation of ammonia-borane ($\text{H}_3\text{N}\cdot\text{BH}_3$) and related amine-borane ($\text{Me}_2\text{HN}\cdot\text{BH}_3$) by $[\text{RuCl}(\text{dppe})_2][\text{OTf}]$ complex (**1**).[89] In these reactions no dissolved NH_3 and Me_2NH were detected, however, we indeed observed the formation of Ru-amine complexes upon B–N bond cleavage.[89] Similarly, complex **1** was also found to be quite reactive towards TBAB and resulted in rapid dehydrogenation along with formation of complexes **2**, **3**, and **4**. More importantly, this reaction showed concomitant elimination of free amine ($^t\text{BuNH}_2$) upon B–N bond cleavage (Figure S10) which facilitates the hydrogenation of CO_2 into formate and then subsequent amidation to formamide in presence of Ru-complexes **2**, **3**, and **4** at relatively low pressure of CO_2 (5-10 bar) and 298 K.

Based on previous reports of carbon dioxide reduction in presence of amines[94][59][95][96][97][52] and our NMR spectroscopic studies, we propose two plausible pathways (i) through carbamate (path A) and (ii) through formic acid or formate (path B) for the transfer hydrogenation and subsequent amidation of CO_2 (Scheme 11). From our spectral data analysis, path B would be more likely, however, path A cannot be ruled out. Further investigations to elucidate a detailed mechanism are in progress.

Scheme 11. Proposed mechanism for amidation of CO_2 using TBAB in presence of complex **1**



Conclusions

In this article, we showed that the five-coordinated and electrophilic $[\text{RuCl}(\text{dppe})_2][\text{OTf}]$ (**1**) complex is moderately reactive towards formic acid and slowly dehydrogenated it under ambient conditions resulting in the formation of *trans*- $[\text{Ru}(\eta^2\text{-H}_2)\text{Cl}(\text{dppe})_2][\text{OTf}]$ (**2**) (major) and *trans*- $[\text{Ru}(\eta^2\text{-H}_2)\text{H}(\text{dppe})_2][\text{OTf}]$ (**3**) (minor). Addition of Hunig base to the reaction mixture resulted in the catalytic dehydrogenation of formic acid and produced quantitative amount of H_2 and CO_2 along with complex **4**. Also, we found that the *cis*- $[\text{Ru}(\eta^2\text{-CF}_3\text{CO}_2)(\text{dppe})_2][\text{OTf}]$ (**6**) complex readily dehydrogenated formic acid leading to complex **3**. Further, we demonstrated the transfer hydrogenation and subsequent amidation of CO_2 by complex **1** in presence of tert-butyl amine-borane. Based on NMR spectroscopic studies, control experiments and previous reports, plausible mechanisms for formic acid dehydrogenation and CO_2 amidation have been proposed. These initial mechanistic insights into mechanism obtained for Ru-complex catalyzed formic acid dehydrogenation and carbon dioxide amidation offer opportunities to further investigate their detailed kinetics and thermodynamics aspects in different solvents using isotopically labelled (DCO_2H) which would lead us to design better performance catalysts.

Experimental Section

General procedures

1 All manipulations were carried out under a dry and oxygen-free N₂ atmosphere using standard Schlenk and
2 inert-atmosphere techniques unless otherwise specified. Reagent-grade solvents (hexanes, petroleum ether,
3 tetrahydrofuran (THF), diethyl ether) were dried and distilled under N₂ atmosphere from Na–benzophenone
4 just before use. Dichloromethane was first dried and distilled over P₂O₅ and then dried and distilled over
5 CaH₂. Methanol was dried and distilled using MgI₂, whereas acetone was dried and distilled over K₂CO₃.
6 Dichloromethane-*d*₂ (CD₂Cl₂) was purchased from Cambridge Isotopes Ltd. USA and distilled over CaH₂
7 before use. [RuCl(dppe)₂][OTf] (**1**) was prepared using the reported method[98] and [Ru(η²-
8 CF₃CO₂)(dppe)₂][OTf] (**6**) was synthesized using complex **1** and silver trifluoroacetate (AgCO₂CF₃,
9 purchased from Sigma-Aldrich). Formic acid (HCO₂H, FA) and tert-butyl amine-borane (^tBuH₂N·BH₃,
10 TBAB) were purchased from Sigma-Aldrich and used as received. NaBH₄ and Hunig base (HB) were
11 purchased from S.D. Fine Chemicals Pvt. Ltd., India and CO₂ (99.95%) from Bhuruka Gas Pvt. Ltd., India.
12 The ¹H, ³¹P{¹H}, ¹³C and ¹⁹F NMR spectral data were obtained using an Avance Bruker 400 MHz
13 spectrometer. The ¹H and ¹³C NMR spectra were referenced using the residual proton signal and ¹³C signal
14 of CD₂Cl₂, respectively. Whenever CH₂Cl₂ was used for the reactions, appropriate quantity of CD₂Cl₂ was
15 added to the sample to obtain the NMR spectra. The ³¹P{¹H} NMR spectra were recorded relative to 85%
16 H₃PO₄(aqueous solution) as an external standard and ¹⁹F NMR spectral signals were referenced using
17 CFCl₃.

18 (i) Dehydrogenation of formic acid by [RuCl(dppe)₂][OTf] complex (**1**)

19 In a 5 mm pressure stable NMR tube, complex **1** (~11 mg, 0.01 mmol) was dissolved in 0.5 mL of dry and
20 distilled CD₂Cl₂. HCO₂H (10 μL, ~0.26 mmol) was added to it and immediately capped with a septum. It
21 was shaken for nearly 10-15 min. During this time, solution turned from dark red to orange and then finally
22 to pale yellow. No gas evolution was noted. The ¹H and ³¹P{¹H} NMR spectra were recorded with time
23 which showed intermediates en route to the final products *trans*-[Ru(η²-H₂)Cl(dppe)₂][OTf] (**2**) and *trans*-
24 [Ru(η²-H₂)H(dppe)₂][OTf] (**3**). Same reaction was carried out in presence of excess non-nucleophilic base
25 (proton sponge), Hunig base (ⁱPr₂NEt, HB, 50-100 μL, ~0.3-0.6 mmol), and in this case continuous gas (H₂
26 + CO₂) evolution was observed even after five runs of HCO₂H dehydrogenation at 298 K accompanied by
27 formation of *trans*-[RuHCl(dppe)₂] complex (**4**) as final product.

28 (ii) Measurement of evolved H₂ and CO₂ gases from catalytic dehydrogenation of formic acid by 29 complex **1**

30 To a two neck Schlenk round bottomed flask was attached a gas burette (filled with water); the flask was
31 charged with complex **1** (~6 mg, 0.005 mmol) and dissolved in 2.0 mL of dichloromethane. HCO₂H (~20
32 μL, ~0.52 mmol) was added to it through a septum using a syringe. It was stirred continuously and

prominent color changes from dark red to orange and then finally to pale yellow were noted. Gas evolution was apparent in the form of downward displacement of water in the burette with time. The rate of gas evolution was very slow initially, however, addition of Hunig base (100 μ L, 0.60 mmol) led to vigorous gas bubbling. The volume of gas evolved was measured for four consecutive runs using formic acid-Hunig base (FAHB) salt [FA (~20 μ L, ~0.52 mmol) and HB (~100 μ L, ~0.60 mmol)] in dichloromethane at room temperature.

Note: Catalytic dehydrogenation was observed only in presence of Hunig base.

(iii) Synthesis of *cis*-[Ru(η^2 -CF₃CO₂)(dppe)₂][OTf] (**6**) complex and its reaction with HCO₂H

In a 5 mm NMR tube, complex **1** (~11 mg, 0.01 mmol) and silver trifluoroacetate (~2.5 mg, ~0.01 mmol) were dissolved in 0.5 mL of CD₂Cl₂. It was shaken for ~5 min, the color turned from dark red to yellow accompanied by precipitation of a white residue at the bottom of the NMR tube. The ¹H, ³¹P{¹H}, and ¹⁹F NMR spectra (Figures S5 & S6) were recorded which revealed the formation of *cis*-[Ru(η^2 -CF₃CO₂)(dppe)₂][OTf] (**6**). Complex **6** was reacted with formic acid (10 μ L, 0.26 mmol) in CH₂Cl₂ which resulted in a color change from intense yellow to pale yellow. The ¹H, and ³¹P{¹H} NMR spectral data showed dehydrogenation of formic acid along with formation of *trans*-[Ru(η^2 -H₂)H(dppe)₂][OTf] (**3**) complex (see SI for details).

(iv) Amidation of CO₂ using [RuCl(dppe)₂][OTf] complex (**1**) in presence of ^tBuH₂N·BH₃

In a pressure stable NMR tube, complex **1** (~11 mg, 0.01 mmol) and ^tBuH₂N·BH₃ (~10 mg, 0.11 mmol) were dissolved in 0.5 mL of CH₂Cl₂ at 298 K. Vigorous gas evolution was observed and the NMR tube was immediately capped. Then, 5-10 bar of CO₂ was pressurized using a high-pressure Swagelok set up and stirred overnight. The ¹H, ³¹P{¹H}, and ¹³CNMR spectra were recorded which showed N-tert-butyl formamide and *trans*-[Ru(η^2 -H₂)H(dppe)₂][OTf] (**3**) and *trans*-[Ru(H)(Cl)(dppe)₂][OTf] complexes (**4**).

Conflicts of interest

There are no conflicts to declare.

Acknowledgements

I acknowledge financial support from Integrated PhD fellowship (Chemical Sciences Division) of Indian Institute of Science (IISc), Bangalore. I also acknowledge Prof. B. R. Jagirdar for discussion and allowing me to use the NMR lab facilities at the Dept. of Inorganic and Physical Chemistry (IISc, Bangalore).

References

- [1] Toward A Hydrogen Economy: Special Section, *Science* (80-.). 305 (2004) 958–976.
- [2] N. Armaroli, V. Balzani, The Future of Energy Supply: Challenges and Opportunities, *Angew. Chemie Int. Ed.* 46 (2007) 52–66. <https://doi.org/https://doi.org/10.1002/anie.200602373>.
- [3] L. Schlapbach, A. Züttel, Hydrogen-storage materials for mobile applications, *Nature*. 414 (2001) 353–358. <https://doi.org/10.1038/35104634>.
- [4] United States. Dept. of Energy. Office of Science, Basic Research Needs for the Hydrogen Economy. Report of the Basic Energy Sciences Workshop on Hydrogen Production, Storage and Use, May 13-15, 2003, Basic Res. Needs Hydrog. Econ. (2004) 178. <http://www.osti.gov/servlets/purl/899224-3RdCK/>.
- [5] A. Staubitz, A.P.M. Robertson, M.E. Sloan, I. Manners, Amine– and Phosphine–Borane Adducts: New Interest in Old Molecules, *Chem. Rev.* 110 (2010) 4023–4078. <https://doi.org/10.1021/cr100105a>.
- [6] A. Staubitz, A.P.M. Robertson, I. Manners, Ammonia-Borane and Related Compounds as Dihydrogen Sources, *Chem. Rev.* 110 (2010) 4079–4124. <https://doi.org/10.1021/cr100088b>.
- [7] T.C. Johnson, D.J. Morris, M. Wills, Hydrogen generation from formic acid and alcohols using homogeneous catalysts, *Chem. Soc. Rev.* 39 (2010) 81–88. <https://doi.org/10.1039/B904495G>.
- [8] M. Yadav, Q. Xu, Liquid-phase chemical hydrogen storage materials, *Energy Environ. Sci.* 5 (2012) 9698–9725. <https://doi.org/10.1039/C2EE22937D>.
- [9] J. Eppinger, K.-W. Huang, Formic Acid as a Hydrogen Energy Carrier, *ACS Energy Lett.* 2 (2017) 188–195. <https://doi.org/10.1021/acsenergylett.6b00574>.
- [10] P.G. Alsabeh, D. Mellmann, H. Junge, M. Beller, Ruthenium-Catalyzed Hydrogen Generation from Alcohols and Formic Acid, Including Ru-Pincer-Type Complexes BT - Ruthenium in Catalysis, in: P.H. Dixneuf, C. Bruneau (Eds.), Springer International Publishing, Cham, 2014: pp. 45–79. https://doi.org/10.1007/3418_2014_84.
- [11] S. Moret, P.J. Dyson, G. Laurenczy, Direct synthesis of formic acid from carbon dioxide by hydrogenation in acidic media, *Nat. Commun.* 5 (2014) 4017. <https://doi.org/10.1038/ncomms5017>.
- [12] P.G. Jessop, T. Ikariya, R. Noyori, Homogeneous catalytic hydrogenation of supercritical carbon dioxide, *Nature*. 368 (1994) 231–233. <https://doi.org/10.1038/368231a0>.

- [13] Y. Manaka, W.-H. Wang, Y. Suna, H. Kambayashi, J.T. Muckerman, E. Fujita, Y. Himeda, Efficient H₂ generation from formic acid using azole complexes in water, *Catal. Sci. Technol.* 4 (2014) 34–37. <https://doi.org/10.1039/C3CY00830D>.
- [14] P.G. Jessop, F. Joó, C.-C. Tai, Recent advances in the homogeneous hydrogenation of carbon dioxide, *Coord. Chem. Rev.* 248 (2004) 2425–2442. <https://doi.org/10.1016/j.ccr.2004.05.019>.
- [15] C. Fellay, P.J. Dyson, G. Laurenczy, A Viable Hydrogen-Storage System Based On Selective Formic Acid Decomposition with a Ruthenium Catalyst, *Angew. Chemie Int. Ed.* 47 (2008) 3966–3968. <https://doi.org/10.1002/anie.200800320>.
- [16] B. Loges, A. Boddien, H. Junge, M. Beller, Controlled Generation of Hydrogen from Formic Acid Amine Adducts at Room Temperature and Application in H₂/O₂ Fuel Cells, *Angew. Chemie Int. Ed.* 47 (2008) 3962–3965. <https://doi.org/10.1002/anie.200705972>.
- [17] A. Boddien, B. Loges, F. Gärtner, C. Torborg, K. Fumino, H. Junge, R. Ludwig, M. Beller, Iron-Catalyzed Hydrogen Production from Formic Acid, *J. Am. Chem. Soc.* 132 (2010) 8924–8934. <https://doi.org/10.1021/ja100925n>.
- [18] A. Boddien, D. Mellmann, F. Gärtner, R. Jackstell, H. Junge, P.J. Dyson, G. Laurenczy, R. Ludwig, M. Beller, Efficient Dehydrogenation of Formic Acid Using an Iron Catalyst, *Science* (80-.). 333 (2011) 1733 LP – 1736. <https://doi.org/10.1126/science.1206613>.
- [19] W. Gan, D.J.M. Snelders, P.J. Dyson, G. Laurenczy, Ruthenium(II)-Catalyzed Hydrogen Generation from Formic Acid using Cationic, Ammoniomethyl-Substituted Triarylphosphine Ligands, *ChemCatChem.* 5 (2013) 1126–1132. <https://doi.org/10.1002/cctc.201200782>.
- [20] Y. Himeda, Highly efficient hydrogen evolution by decomposition of formic acid using an iridium catalyst with 4,4'-dihydroxy-2,2'-bipyridine, *Green Chem.* 11 (2009) 2018–2022. <https://doi.org/10.1039/B914442K>.
- [21] C. Guan, D.-D. Zhang, Y. Pan, M. Iguchi, M.J. Ajitha, J. Hu, H. Li, C. Yao, M.-H. Huang, S. Min, J. Zheng, Y. Himeda, H. Kawanami, K.-W. Huang, Dehydrogenation of Formic Acid Catalyzed by a Ruthenium Complex with an N,N'-Diimine Ligand, *Inorg. Chem.* 56 (2017) 438–445. <https://doi.org/10.1021/acs.inorgchem.6b02334>.
- [22] P. Stathi, M. Solakidou, M. Louloudi, Y. Deligiannakis, From Homogeneous to Heterogenized Molecular Catalysts for H₂ Production by Formic Acid Dehydrogenation: Mechanistic Aspects, Role of Additives, and Co-Catalysts, *Energies* . 13 (2020). <https://doi.org/10.3390/en13030733>.
- [23] H. Liu, W.-H. Wang, H. Xiong, A. Nijamudheen, M.Z. Ertem, M. Wang, L. Duan, Efficient Iridium Catalysts for Formic Acid Dehydrogenation: Investigating the Electronic Effect on the Elementary β -Hydride Elimination and Hydrogen Formation Steps, *Inorg. Chem.* 60 (2021) 3410–

3417. <https://doi.org/10.1021/acs.inorgchem.0c03815>.

[24] S. Patra, S.K. Singh, Hydrogen Production from Formic Acid and Formaldehyde over Ruthenium Catalysts in Water, *Inorg. Chem.* 59 (2020) 4234–4243. <https://doi.org/10.1021/acs.inorgchem.9b02882>.

[25] S.M. Barrett, S.A. Slattery, A.J.M. Miller, Photochemical Formic Acid Dehydrogenation by Iridium Complexes: Understanding Mechanism and Overcoming Deactivation, *ACS Catal.* 5 (2015) 6320–6327. <https://doi.org/10.1021/acscatal.5b01995>.

[26] I. Mellone, F. Bertini, M. Peruzzini, L. Gonsalvi, An active, stable and recyclable Ru(ii) tetraphosphine-based catalytic system for hydrogen production by selective formic acid dehydrogenation, *Catal. Sci. Technol.* 6 (2016) 6504–6512. <https://doi.org/10.1039/C6CY01219A>.

[27] E.A. Bielinski, P.O. Lagaditis, Y. Zhang, B.Q. Mercado, C. Würtele, W.H. Bernskoetter, N. Hazari, S. Schneider, Lewis Acid-Assisted Formic Acid Dehydrogenation Using a Pincer-Supported Iron Catalyst, *J. Am. Chem. Soc.* 136 (2014) 10234–10237. <https://doi.org/10.1021/ja505241x>.

[28] M. Grasemann, G. Laurenczy, Formic acid as a hydrogen source – recent developments and future trends, *Energy Environ. Sci.* 5 (2012) 8171–8181. <https://doi.org/10.1039/C2EE21928J>.

[29] J.J.A. Celaje, Z. Lu, E.A. Kedzie, N.J. Terrile, J.N. Lo, T.J. Williams, A prolific catalyst for dehydrogenation of neat formic acid, *Nat. Commun.* 7 (2016) 11308. <https://doi.org/10.1038/ncomms11308>.

[30] K. Sordakis, M. Beller, G. Laurenczy, Chemical Equilibria in Formic Acid/Amine-CO₂ Cycles under Isochoric Conditions using a Ruthenium(II) 1,2-Bis(diphenylphosphino)ethane Catalyst, *ChemCatChem*. 6 (2014) 96–99. <https://doi.org/10.1002/cctc.201300740>.

[31] N. Lentz, A. Aloisi, P. Thuéry, E. Nicolas, T. Cantat, Additive-Free Formic Acid Dehydrogenation Catalyzed by a Cobalt Complex, *Organometallics*. 40 (2021) 565–569. <https://doi.org/10.1021/acs.organomet.0c00777>.

[32] C. Guan, Y. Pan, T. Zhang, M.J. Ajitha, K.-W. Huang, An Update on Formic Acid Dehydrogenation by Homogeneous Catalysis, *Chem. – An Asian J.* 15 (2020) 937–946. <https://doi.org/10.1002/asia.201901676>.

[33] C. Prichatz, M. Trincado, L. Tan, F. Casas, A. Kammer, H. Junge, M. Beller, H. Grützmacher, Highly Efficient Base-Free Dehydrogenation of Formic Acid at Low Temperature, *ChemSusChem*. 11 (2018) 3092–3095. <https://doi.org/10.1002/cssc.201801072>.

[34] A. Thevenon, E. Frost-Pennington, G. Weijia, A.F. Dalebrook, G. Laurenczy, Formic Acid Dehydrogenation Catalysed by Tris(TPPTS) Ruthenium Species: Mechanism of the Initial “Fast”

Cycle, ChemCatChem. 6 (2014) 3146–3152.

<https://doi.org/https://doi.org/10.1002/cctc.201402410>.

[35] J. Lücken, T. Auth, S.I. Mozzi, F. Meyer, Hexanuclear Copper(I) Hydride from the Reduction-Induced Decarboxylation of a Dicopper(II) Formate, *Inorg. Chem.* 59 (2020) 14347–14354. <https://doi.org/10.1021/acs.inorgchem.0c02126>.

[36] I. Mellone, M. Peruzzini, L. Rosi, D. Mellmann, H. Junge, M. Beller, L. Gonsalvi, Formic acid dehydrogenation catalysed by ruthenium complexes bearing the tripodal ligands triphos and NP3, *Dalt. Trans.* 42 (2013) 2495–2501. <https://doi.org/10.1039/C2DT32043F>.

[37] A. Léval, H. Junge, M. Beller, Manganese(i) κ^2 -NN complex-catalyzed formic acid dehydrogenation, *Catal. Sci. Technol.* 10 (2020) 3931–3937. <https://doi.org/10.1039/D0CY00769B>.

[38] A. Léval, H. Junge, M. Beller, Formic Acid Dehydrogenation by a Cyclometalated κ^3 -CNN Ruthenium Complex, *Eur. J. Inorg. Chem.* 2020 (2020) 1293–1299. <https://doi.org/https://doi.org/10.1002/ejic.202000068>.

[39] D. Hong, Y. Shimoyama, Y. Ohgomori, R. Kanega, H. Kotani, T. Ishizuka, Y. Kon, Y. Himeda, T. Kojima, Cooperative Effects of Heterodinuclear IrIII–MII Complexes on Catalytic H₂ Evolution from Formic Acid Dehydrogenation in Water, *Inorg. Chem.* 59 (2020) 11976–11985. <https://doi.org/10.1021/acs.inorgchem.0c00812>.

[40] N. Onishi, M. Iguchi, X. Yang, R. Kanega, H. Kawanami, Q. Xu, Y. Himeda, Development of Effective Catalysts for Hydrogen Storage Technology Using Formic Acid, *Adv. Energy Mater.* 9 (2019) 1801275. <https://doi.org/https://doi.org/10.1002/aenm.201801275>.

[41] A. Léval, A. Agapova, C. Steinlechner, E. Alberico, H. Junge, M. Beller, Hydrogen production from formic acid catalyzed by a phosphine free manganese complex: investigation and mechanistic insights, *Green Chem.* 22 (2020) 913–920. <https://doi.org/10.1039/C9GC02453K>.

[42] D. Mellmann, P. Sponholz, H. Junge, M. Beller, Formic acid as a hydrogen storage material – development of homogeneous catalysts for selective hydrogen release, *Chem. Soc. Rev.* 45 (2016) 3954–3988. <https://doi.org/10.1039/C5CS00618J>.

[43] K. Grubel, H. Jeong, C.W. Yoon, T. Autrey, Challenges and opportunities for using formate to store, transport, and use hydrogen, *J. Energy Chem.* 41 (2020) 216–224. <https://doi.org/https://doi.org/10.1016/j.jechem.2019.05.016>.

[44] X. Yang, Mechanistic insights into iron catalyzed dehydrogenation of formic acid: β -hydride elimination vs. direct hydride transfer, *Dalt. Trans.* 42 (2013) 11987–11991. <https://doi.org/10.1039/C3DT50908G>.

- 1 [45] D.J. Morris, G.J. Clarkson, M. Wills, Insights into Hydrogen Generation from Formic Acid Using
2 Ruthenium Complexes, *Organometallics*. 28 (2009) 4133–4140.
3 <https://doi.org/10.1021/om900099u>.
- 4 [46] T. Schaub, R.A. Paciello, A Process for the Synthesis of Formic Acid by CO₂ Hydrogenation:
5 Thermodynamic Aspects and the Role of CO, *Angew. Chemie Int. Ed.* 50 (2011) 7278–7282.
6 <https://doi.org/https://doi.org/10.1002/anie.201101292>.
- 7 [47] C. Ziebart, C. Federsel, P. Anbarasan, R. Jackstell, W. Baumann, A. Spannenberg, M. Beller,
8 Well-Defined Iron Catalyst for Improved Hydrogenation of Carbon Dioxide and Bicarbonate, *J.*
9 *Am. Chem. Soc.* 134 (2012) 20701–20704. <https://doi.org/10.1021/ja307924a>.
- 10 [48] L.M. Potter, Sean, Michael Cabbage, press release/nasa-noaa data show 2016 warmest year on
11 record globally, NASA/NOAA Webpage. (2017). [https://www.nasa.gov/press-release/nasa-noaa-](https://www.nasa.gov/press-release/nasa-noaa-data-show-2016-warmest-year-on-record-globally)
12 [data-show-2016-warmest-year-on-record-globally](https://www.nasa.gov/press-release/nasa-noaa-data-show-2016-warmest-year-on-record-globally).
- 13 [49] Trends in Atmospheric Carbon Dioxide, *Glob. Monit. Lab. Earth Syst. Res. Lab. NOAA*. (2021).
14 <https://www.esrl.noaa.gov/gmd/ccgg/trends/>.
- 15 [50] IPCC, Climate Change 2001: Synthesis Report, (2001).
16 <https://archive.ipcc.ch/ipccreports/tar/vol4/index.php?idp=27>.
- 17 [51] L.B. Maia, I. Moura, J.J.G. Moura, Carbon Dioxide Utilisation—The Formate Route BT -
18 Enzymes for Solving Humankind’s Problems: Natural and Artificial Systems in Health,
19 Agriculture, Environment and Energy, in: J.J.G. Moura, I. Moura, L.B. Maia (Eds.), Springer
20 International Publishing, Cham, 2021: pp. 29–81. https://doi.org/10.1007/978-3-030-58315-6_2.
- 21 [52] P.G. Jessop, T. Ikariya, R. Noyori, Homogeneous Hydrogenation of Carbon Dioxide, *Chem. Rev.*
22 95 (1995) 259–272. <https://doi.org/10.1021/cr00034a001>.
- 23 [53] G. Centi, S. Perathoner, Opportunities and prospects in the chemical recycling of carbon dioxide to
24 fuels, *Catal. Today*. 148 (2009) 191–205.
25 <https://doi.org/https://doi.org/10.1016/j.cattod.2009.07.075>.
- 26 [54] M.Aresta, Carbon Dioxide Recovery and Utilization, Springer Netherlands, 2003.
27 <https://doi.org/10.1007/978-94-017-0245-4>.
- 28 [55] M.L. and L.M. Bert Metz, Ogunlade Davidson, Heleen de Coninck, Carbon Dioxide Capture and
29 Storage, 2005. <https://www.ipcc.ch/report/carbon-dioxide-capture-and-storage/>.
- 30 [56] Y. Himeda, M. Beller, W.-H. Wang, X. Feng, M. Bao, L. Gonsalvi, A. Guerriero, S. Kostera, S.
31 Kar, A. Goeppert, G.K. Surya Prakash, X. Yan, X. Yang, K. Park, G.H. Gunasekar, S. Yoon, K.
32 Mori, H. Yamashita, N. Phongprueksathat, A. Urakawa, C.R. Carr, L.A. Berben, N. Onishi, Y.
33 Himeda, *Front Matter, CO₂ Hydrog. Catal.* (2021) i–xi.

<https://doi.org/https://doi.org/10.1002/9783527824113.fmatter>.

[57] A.L. Dzubak, L.-C. Lin, J. Kim, J.A. Swisher, R. Poloni, S.N. Maximoff, B. Smit, L. Gagliardi, Ab initio carbon capture in open-site metal–organic frameworks, *Nat. Chem.* 4 (2012) 810–816. <https://doi.org/10.1038/nchem.1432>.

[58] E. Balaraman, C. Gunanathan, J. Zhang, L.J.W. Shimon, D. Milstein, Efficient hydrogenation of organic carbonates, carbamates and formates indicates alternative routes to methanol based on CO₂ and CO, *Nat. Chem.* 3 (2011) 609–614. <https://doi.org/10.1038/nchem.1089>.

[59] A.D. Getty, C.-C. Tai, J.C. Linehan, P.G. Jessop, M.M. Olmstead, A.L. Rheingold, Hydrogenation of Carbon Dioxide Catalyzed by Ruthenium Trimethylphosphine Complexes: A Mechanistic Investigation Using High-Pressure NMR Spectroscopy, *Organometallics*. 28 (2009) 5466–5477. <https://doi.org/10.1021/om900128s>.

[60] P. Munshi, A.D. Main, J.C. Linehan, C.-C. Tai, P.G. Jessop, Hydrogenation of Carbon Dioxide Catalyzed by Ruthenium Trimethylphosphine Complexes: The Accelerating Effect of Certain Alcohols and Amines, *J. Am. Chem. Soc.* 124 (2002) 7963–7971. <https://doi.org/10.1021/ja0167856>.

[61] C.-C. Tai, J. Pitts, J.C. Linehan, A.D. Main, P. Munshi, P.G. Jessop, In Situ Formation of Ruthenium Catalysts for the Homogeneous Hydrogenation of Carbon Dioxide, *Inorg. Chem.* 41 (2002) 1606–1614. <https://doi.org/10.1021/ic010866l>.

[62] L.-C. Lin, A.H. Berger, R.L. Martin, J. Kim, J.A. Swisher, K. Jariwala, C.H. Rycroft, A.S. Bhowan, M.W. Deem, M. Haranczyk, B. Smit, In silico screening of carbon-capture materials, *Nat. Mater.* 11 (2012) 633–641. <https://doi.org/10.1038/nmat3336>.

[63] J.D. Erickson, A.Z. Preston, J.C. Linehan, E.S. Wiedner, Enhanced Hydrogenation of Carbon Dioxide to Methanol by a Ruthenium Complex with a Charged Outer-Coordination Sphere, *ACS Catal.* 10 (2020) 7419–7423. <https://doi.org/10.1021/acscatal.0c02268>.

[64] G.A. Olah, A. Goeppert, G.K.S. Prakash, *Beyond Oil and Gas: The Methanol Economy: Second Edition*, 2nd edn, Wiley-VCH, Weinheim, Germany, 2009. <https://doi.org/10.1002/9783527627806>.

[65] A. Goeppert, M. Czaun, J.-P. Jones, G.K. Surya Prakash, G.A. Olah, Recycling of carbon dioxide to methanol and derived products – closing the loop, *Chem. Soc. Rev.* 43 (2014) 7995–8048. <https://doi.org/10.1039/C4CS00122B>.

[66] W.-H. Wang, Y. Himeda, J.T. Muckerman, G.F. Manbeck, E. Fujita, CO₂ Hydrogenation to Formate and Methanol as an Alternative to Photo- and Electrochemical CO₂ Reduction, *Chem. Rev.* 115 (2015) 12936–12973. <https://doi.org/10.1021/acs.chemrev.5b00197>.

- 1 [67] M.S. Jeletic, M.T. Mock, A.M. Appel, J.C. Linehan, A Cobalt-Based Catalyst for the
2 Hydrogenation of CO₂ under Ambient Conditions, *J. Am. Chem. Soc.* 135 (2013) 11533–11536.
3 <https://doi.org/10.1021/ja406601v>.
- 4 [68] Y. Musashi, S. Sakaki, Theoretical Study of Ruthenium-Catalyzed Hydrogenation of Carbon
5 Dioxide into Formic Acid. Reaction Mechanism Involving a New Type of σ -Bond Metathesis, *J.*
6 *Am. Chem. Soc.* 122 (2000) 3867–3877. <https://doi.org/10.1021/ja9938027>.
- 7 [69] F. Liu, M.B. Abrams, R.T. Baker, W. Tumas, Phase-separable catalysis using room temperature
8 ionic liquids and supercritical carbon dioxide, *Chem. Commun.* (2001) 433–434.
9 <https://doi.org/10.1039/B009701M>.
- 10 [70] O. Kröcher, R. A. Köppel, A. Baiker, Highly active ruthenium complexes with bidentate phosphine
11 ligands for the solvent-free catalytic synthesis of N,N-dimethylformamide and methyl formate,
12 *Chem. Commun.* (1997) 453–454. <https://doi.org/10.1039/A608150I>.
- 13 [71] L. Cervený, *Catalytic Hydrogenation*, Elsevier, Amsterdam, 1986.
- 14 [72] J.G. de V. and C.J. Elsevier, *The Handbook of Homogeneous Hydrogenation*, Wiley-VCH,
15 Weinheim, Germany, 2007.
- 16 [73] P.G.A. and I.J. Munslow, *Modern Reduction Methods*, Wiley-VCH Verlag GmbH & Co. KGaA,
17 Weinheim, Germany, 2008.
- 18 [74] G. Brieger, T.J. Nestrick, Catalytic transfer hydrogenation, *Chem. Rev.* 74 (1974) 567–580.
19 <https://doi.org/10.1021/cr60291a003>.
- 20 [75] R.A.W. Johnstone, A.H. Wilby, I.D. Entwistle, Heterogeneous catalytic transfer hydrogenation and
21 its relation to other methods for reduction of organic compounds, *Chem. Rev.* 85 (1985) 129–170.
22 <https://doi.org/10.1021/cr00066a003>.
- 23 [76] X. Wu, J. Xiao, Aqueous-phase asymmetric transfer hydrogenation of ketones – a greener
24 approach to chiral alcohols, *Chem. Commun.* (2007) 2449–2466.
25 <https://doi.org/10.1039/B618340A>.
- 26 [77] S. Gladiali, E. Alberico, Asymmetric transfer hydrogenation: chiral ligands and applications,
27 *Chem. Soc. Rev.* 35 (2006) 226–236. <https://doi.org/10.1039/B513396C>.
- 28 [78] S.E. Clapham, A. Hadzovic, R.H. Morris, Mechanisms of the H₂-hydrogenation and transfer
29 hydrogenation of polar bonds catalyzed by ruthenium hydride complexes, *Coord. Chem. Rev.* 248
30 (2004) 2201–2237. <https://doi.org/https://doi.org/10.1016/j.ccr.2004.04.007>.
- 31 [79] M.J. Palmer, M. Wills, Asymmetric transfer hydrogenation of C=O and C=N bonds, *Tetrahedron:*
32 *Asymmetry*. 10 (1999) 2045–2061. [https://doi.org/https://doi.org/10.1016/S0957-4166\(99\)00216-](https://doi.org/https://doi.org/10.1016/S0957-4166(99)00216-)

- [80] R. Noyori, S. Hashiguchi, Asymmetric Transfer Hydrogenation Catalyzed by Chiral Ruthenium Complexes, *Acc. Chem. Res.* 30 (1997) 97–102. <https://doi.org/10.1021/ar9502341>.
- [81] C. Wang, X. Wu, J. Xiao, Broader, Greener, and More Efficient: Recent Advances in Asymmetric Transfer Hydrogenation, *Chem. – An Asian J.* 3 (2008) 1750–1770. <https://doi.org/10.1002/asia.200800196>.
- [82] K. Everaere, A. Mortreux, J.-F. Carpentier, Ruthenium(II)-Catalyzed Asymmetric Transfer Hydrogenation of Carbonyl Compounds with 2-Propanol and Ephedrine-Type Ligands, *Adv. Synth. Catal.* 345 (2003) 67–77. <https://doi.org/10.1002/adsc.200390030>.
- [83] G. Zassinovich, G. Mestroni, S. Gladiali, Asymmetric hydrogen transfer reactions promoted by homogeneous transition metal catalysts, *Chem. Rev.* 92 (1992) 1051–1069. <https://doi.org/10.1021/cr00013a015>.
- [84] T. Ikariya, A.J. Blacker, Asymmetric Transfer Hydrogenation of Ketones with Bifunctional Transition Metal-Based Molecular Catalysts, *Acc. Chem. Res.* 40 (2007) 1300–1308. <https://doi.org/10.1021/ar700134q>.
- [85] G. Ménard, D.W. Stephan, CO₂ reduction via aluminum complexes of ammonia boranes, *Dalt. Trans.* 42 (2013) 5447–5453. <https://doi.org/10.1039/C3DT00098B>.
- [86] G. Ménard, D.W. Stephan, Room Temperature Reduction of CO₂ to Methanol by Al-Based Frustrated Lewis Pairs and Ammonia Borane, *J. Am. Chem. Soc.* 132 (2010) 1796–1797. <https://doi.org/10.1021/ja9104792>.
- [87] Y. Pan, C.-L. Pan, Y. Zhang, H. Li, S. Min, X. Guo, B. Zheng, H. Chen, A. Anders, Z. Lai, J. Zheng, K.-W. Huang, Selective Hydrogen Generation from Formic Acid with Well-Defined Complexes of Ruthenium and Phosphorus–Nitrogen PN₃-Pincer Ligand, *Chem. – An Asian J.* 11 (2016) 1357–1360. <https://doi.org/10.1002/asia.201600169>.
- [88] B. Chin, A.J. Lough, R.H. Morris, C.T. Schweitzer, C. D’Agostino, Influence of Chloride versus Hydride on H–H Bonding and Acidity of the Trans Dihydrogen Ligand in the Complexes trans-[Ru(H₂)X(PR₂CH₂CH₂PR₂)₂]⁺, X = Cl, H, R = Ph, Et. Crystal Structure Determinations of [RuCl(dppe)₂]PF₆ and trans-[Ru(H₂)Cl(dppe)₂]PF₆, *Inorg. Chem.* 33 (1994) 6278–6288. <https://doi.org/10.1021/ic00104a043>.
- [89] R. Kumar, B.R. Jagirdar, B–H Bond Activation Using an Electrophilic Metal Complex: Insights into the Reaction Pathway, *Inorg. Chem.* 52 (2013) 28–36. <https://doi.org/10.1021/ic300390s>.
- [90] R. Kumar, S. Ramakrishnan, E.D. Jemmis, B.R. Jagirdar, Implication of a σ -Methane Complex en Route to Elimination of Methane from a Ruthenium Complex: An Experimental and Theoretical

Investigation, *Organometallics*. 34 (2015) 1245–1254. <https://doi.org/10.1021/om501248v>.

[91] M.T. Bautista, E.P. Cappellani, S.D. Drouin, R.H. Morris, C.T. Schweitzer, A. Sella, J. Zubkowski, Preparation and spectroscopic properties of the η^2 -dihydrogen complexes $[\text{MH}(\eta^2\text{-H}_2)\text{PR}_2\text{CH}_2\text{CH}_2\text{PR}_2)_2] + (\text{M} = \text{iron, ruthenium; R} = \text{Ph, Et})$ and trends in properties down the iron group triad, *J. Am. Chem. Soc.* 113 (1991) 4876–4887. <https://doi.org/10.1021/ja00013a025>.

[92] S.P. Nolan, T.R. Belderrain, R.H. Grubbs, Convenient Synthesis of Ruthenium(II) Dihydride Phosphine Complexes $\text{Ru}(\text{H})_2(\text{PP})_2$ and $\text{Ru}(\text{H})_2(\text{PR}_3)_x$ ($x = 3$ and 4), *Organometallics*. 16 (1997) 5569–5571. <https://doi.org/10.1021/om9706673>.

[93] E.B. Boyar, P.A. Harding, S.D. Robinson, C.P. Brock, Complexes of the platinum metals. Part 31. Reactions of binuclear ruthenium(II,III) and rhodium(II) carboxylates with chelating diphosphines; X-ray crystal structure of (acetato- O, O')bis[bis(diphenylphosphino)methane- P, P']ruthenium(II) tetraphenylborate, *J. Chem. Soc. Dalt. Trans.* (1986) 1771–1778. <https://doi.org/10.1039/DT9860001771>.

[94] N.M. Rezayee, C.A. Huff, M.S. Sanford, Tandem Amine and Ruthenium-Catalyzed Hydrogenation of CO_2 to Methanol, *J. Am. Chem. Soc.* 137 (2015) 1028–1031. <https://doi.org/10.1021/ja511329m>.

[95] P. Haynes, L.H. Slaugh, J.F. Kohnle, Formamides from carbon dioxide, amines and hydrogen in the presence of metal complexes, *Tetrahedron Lett.* 11 (1970) 365–368. [https://doi.org/https://doi.org/10.1016/0040-4039\(70\)80086-7](https://doi.org/10.1016/0040-4039(70)80086-7).

[96] M.A. Affan, P.G. Jessop, Catalytic Formylation of Primary and Secondary Amines with CO_2 and H_2 Using Abundant-Metal Catalysts, *Inorg. Chem.* 56 (2017) 7301–7305. <https://doi.org/10.1021/acs.inorgchem.7b01242>.

[97] S. Kar, R. Sen, A. Goeppert, G.K.S. Prakash, Integrative CO_2 Capture and Hydrogenation to Methanol with Reusable Catalyst and Amine: Toward a Carbon Neutral Methanol Economy, *J. Am. Chem. Soc.* 140 (2018) 1580–1583. <https://doi.org/10.1021/jacs.7b12183>.

[98] M.A. Fox, J.E. Harris, S. Heider, V. Pérez-Gregorio, M.E. Zakrzewska, J.D. Farmer, D.S. Yufit, J.A.K. Howard, P.J. Low, A simple synthesis of $\text{trans-RuCl}(\text{CCR})(\text{dppe})_2$ complexes and representative molecular structures, *J. Organomet. Chem.* 694 (2009) 2350–2358. <https://doi.org/https://doi.org/10.1016/j.jorganchem.2009.03.033>.

1 Graphical Abstract

